Preparation of mesoporous activated carbon fiber by steam activation in the presence of cerium oxide and its adsorption of Congo red and Vitamin B12 from solution

WENZHONG SHEN*, JINGTANG ZHENG
State Key Laboratory of Heavy Oil Processing, University of Petroleum, Dongying 257061, People's Republic of China
E-mail: shenwzh2000@yahoo.com

ZHANGFENG QIN, JIANGUO WANG
State Key Laboratory of Coal Conversion, Institute of Coal Chemistry, Chinese Academy of Sciences, Taiyuan 030001, People's Republic of China

YIHONG LIU
State Key Laboratory of Heavy Oil Processing, University of Petroleum, Dongying 257061, People's Republic of China

Activated carbons are widely used in separation and purification processing, and as catalysis supports [1, 2]. Activated carbon fibers (ACFs) as a new type of activated carbon have an excellent adsorptive property due to large specific surface area, pore volume, and uniform microporosity. Generally, the micropore in ACF cannot meet some special demands, such as adsorption of bulky molecules from solution and catalyst supports for macromolecule reaction [3]. So, it is desired to increase the mesopore and macropore content in ACF and exploit its new applications.

Polymer additives or catalyst was added to the carbon source and carbonized to obtain mesoporous carbon fiber; but it was difficult to eliminate the catalyst from the mesoporous carbon fiber matrix [4–6].

The transition metal and rare earth metal compounds can promote the development of mesopores in activated carbon [7–9]. The activation reaction takes place in the immediate vicinity of metal/oxide particles, leading to the formation of mesopores and macrospores by pitting holes into the carbon matrix [10]. Potassium hydrate can promote the mesopore development, but it needs higher loading amount if the post-treatment is complex. Yttrium acetylacetonate [$Y(acac)_3$] was added to the precursor of carbon and used as catalyst to increase the mesopore content of ACF, but the cost was high [11]. Cerium oxide showed certain activity due to its role in the oxidization–reduction cycle [12] and it could promote the mesopore development in activated carbon with scatter pore size distribution due to the original property of activated carbon [13].

In the current work, cerium nitrate was selected to investigate its catalytic effect on the mesopore development of commercial ACF with steam activation. The commercial ACF was first impregnated with the aqueous solution of cerium nitrate. The loadings of cerium nitrate on the basis of activated carbon were 2.0 wt%. The samples were then dried at 110 °C for overnight and calcined at desired temperatures under nitrogen flow. Catalytic steam activation reaction was performed at 680 °C and 740 °C. Finally, the resulting ACFs were cooled down to room temperature in nitrogen and were leached by acid to remove cerium oxide.

The surface area and mesopore structure of the sample were measured by nitrogen adsorption (77 K) on ASAP2000 (Micromeritic). The surface area and mesopore size distributions were calculated by the BET and BJH method, respectively. X-ray powder diffraction patterns were determined at Rigaku diffractometer (D/max 2500) using Cu K_α radiation. The samples were scanned from 10 to 80° (2θ) at the rate of 5°/min. The SEM images of the samples were obtained using a JEOL Electron microscope.

To estimate the applicability of produced ACF as an adsorbent for adsorption from solution, Congo red and VB12 were selected as target molecules to examine the adsorption property of ACF by batch equilibrium technique. Their molecular size is $2.8 \times 1.1 \times 0.5$ nm [14] and $1.83 \times 1.41 \times 1.14$ nm [9], respectively. The initial concentrations were 1.5×10^{-4} M and 7.5×10^{-5} M for Congo red and VB12, respectively. A series of 2×10^{-4} m^3 Congo red containing 3×10^{-4} kg ACF and 2×10^{-4} m^3 VB12 with 1×10^{-4} kg ACF samples were sealed and shaken at room temperature. The VB12 and Congo red were analyzed using 7550 spectrophotometer (Shanghai Analyzer Company, China), with detected characteristic peaks at 361 nm and 488 nm, respectively.

The primary parameters of the samples prepared at different conditions are listed in Table I. The surface area and pore volume were increased after activation. It is evidenced that the mesopore volume increased markedly while the micropore had less changing. The mesopore volume of the sample prepared by steam is lower than that prepared with cerium oxide.

---

*Author to whom all correspondence should be addressed.

0022–2461

TABLE I The primary parameters of samples

Samples	Catalyst	Activation Temperature (°C)	Activation Time (min)	S_{BET} (m^2/g)	V_{total} ($\times10^{-3}$ m^3/kg)	V_{micro} ($\times10^{-3}$ m^3/kg)	V_{meso} ($\times10^{-3}$ m^3/kg)	$V_{\mathrm{meso}}/V_{\mathrm{total}}$ (%)
ACF-0	–	–	–	847	0.4175	0.3406	0.0528	12.64
ACF-1	–	680	600	1008	0.4729	0.3630	0.0833	17.61
ACF-2	–	740	480	1044	0.5191	0.3666	0.1041	20.05
ACF-3	Ce	680	600	1146	0.5915	0.3854	0.1676	28.33
ACF-4	Ce	740	480	1224	0.6360	0.3788	0.2398	37.70

Fig. 1 gives the nitrogen adsorption–desorption isotherms of the samples. The hysteresis loops of H3 type proved the existence of mesopores, which was observed in the case of aggregates of plate-like particles giving rise to slit-shaped pores [15]. The adsorption capacity increases with the activation temperature. At the higher relative pressure, the isotherm of original ACF changes steeply that indicates more macropore existing. However, there has less macropore after activation due to the platter isotherm at higher relative pressure.

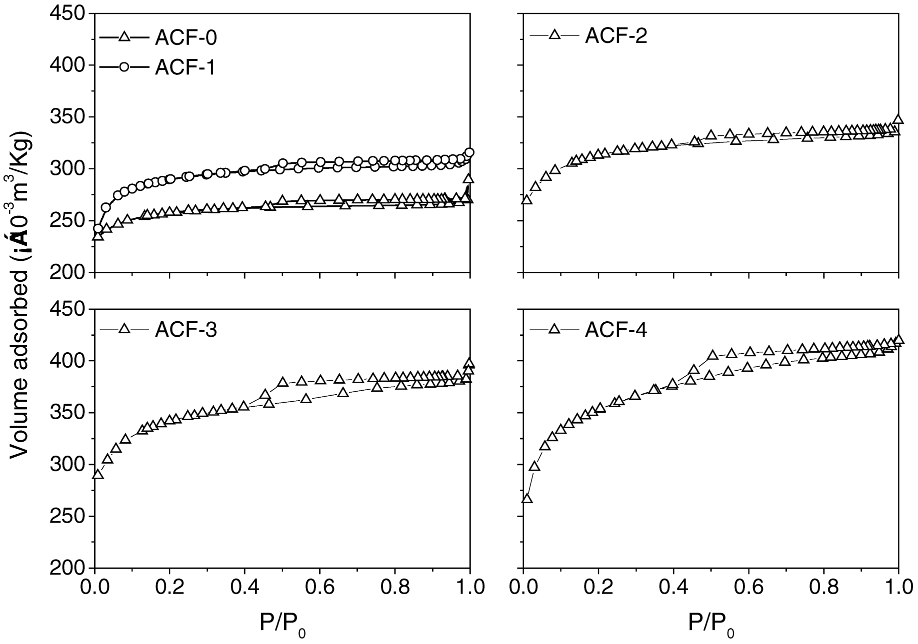

Figure 1 Nitrogen adsorption–desorption isotherms of samples.

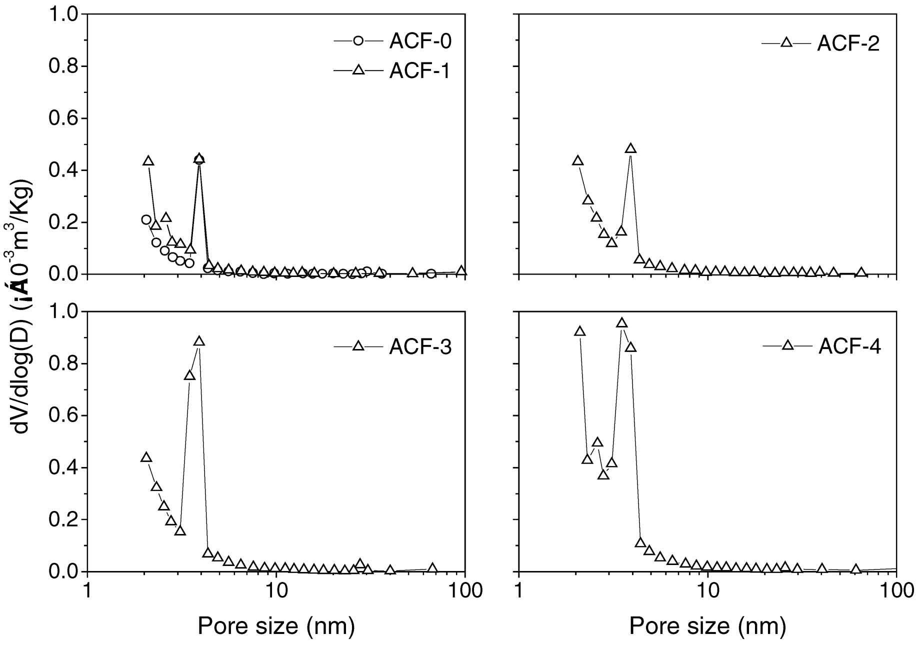

Figure 2 Pore size distribution of samples.

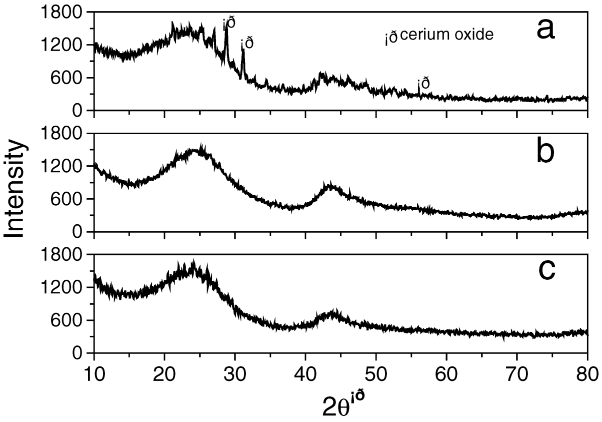

Figure 3 XRD patterns of samples loading of 2.0% cerium nitrate: (a) activated at 740 °C for 480 min, (b) activated at 600 °C for 600 min, and (c) before activation.

The pore size distribution calculated by the BJH method is shown in Fig. 2. The original ACF has less content of mesopore in 3–4 nm; the mesopore distributions of the samples after activation are still in this area except its intensity is much higher. The sample activated without cerium oxide has poorly developed mesopore because the gasification rate of carbon at 680 °C is slow, so the increased mesopore in ACF-3 is mainly resulted from the catalytic activation. When the activation temperature rises up to 740 °C, the non-catalytic activation affects the development of mesopore less than 3 nm in limited. The catalytic activation significantly promotes the development of mesopore in 3–4 nm although it also increases the mesopore volume less than 3 nm. As well as the sample prepared with catalyst at 680 °C has more concentrated pore size distribution in 3–4 nm than that prepared at 740 °C, the catalyst particles have poorer migration trends at 680 °C than that at 740 °C, the catalytic activation takes place around the cerium oxide particle and the mesopore produced with uniform size. However, the catalyst particles will migrate to grow into larger particles and the catalytic activity will decrease at 740 °C; as a result, the mesopore was produced with scatter distribution.

Both catalytic and non-catalytic activation exist during the steam activation process. The rates of the two

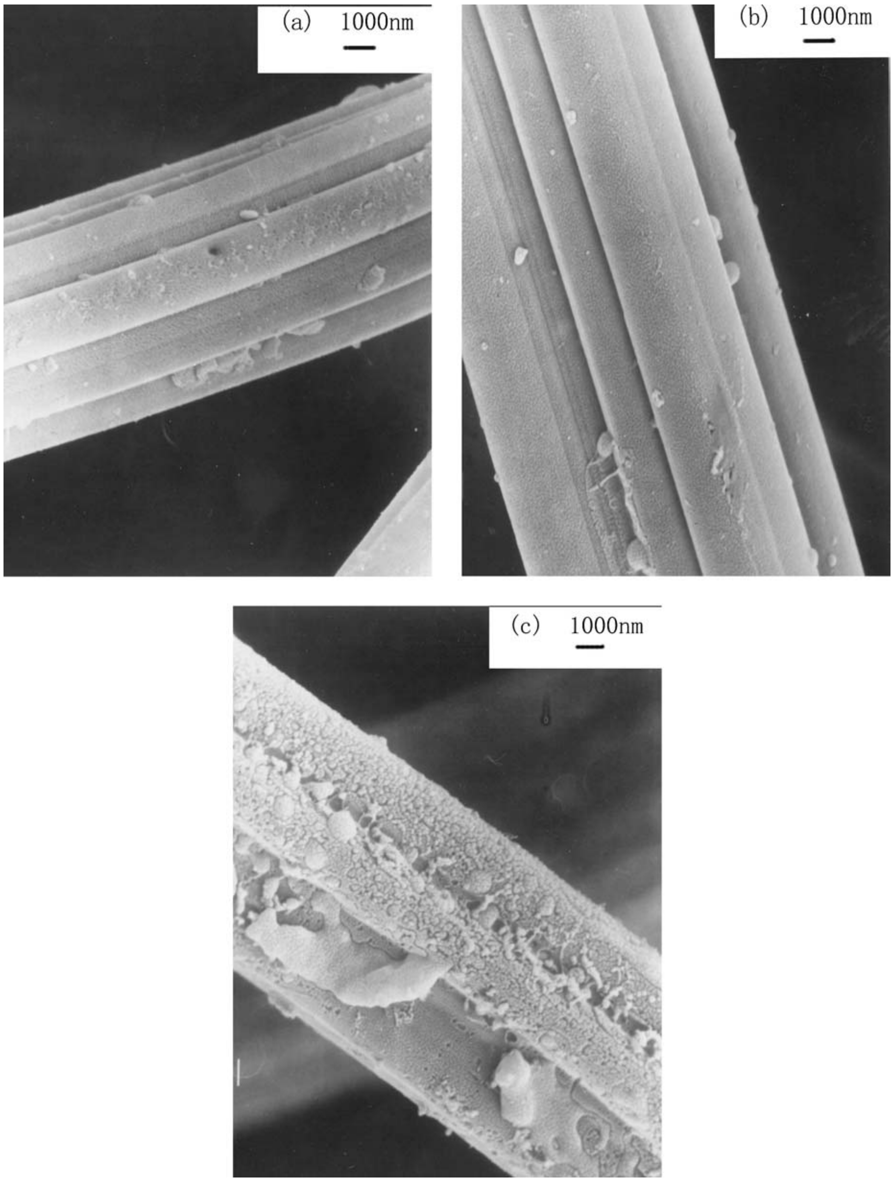

Figure 4 SEM of samples: (a) the original ACF, (b) activated at 740 °C for 480 min without cerium oxide, and (c) activated at 740 °C for 480 min with cerium oxide.

activation reactions increase with temperature. The activation is controlled by chemical reaction at lower temperature; the catalytic activation rate is slower but it takes the dominant role. The mesopore content with relatively concentrated will be increased at a certain degree by prolonging the activation time. However, at high temperature, the activation is controlled by diffusion; the advantage of the catalytic the activation is not significant compared to the non-catalytic activation. The catalytic reaction rate increases, but the metal oxide is also easy to aggregate. Consequently, the metal oxide particles grow into larger ones, which are poorly dispersed and will decrease the catalytic activity.

Fig. 3 shows the X-ray powder diffraction patterns of the sample with 2.0% loading of cerium nitrate before activation, activated at 680 °C for 600 min and 740 °C for 480 min, respectively. The characteristic peaks of cerium oxide, which are at 28.40°, 32.95°, 47.35°, and 56.25°, corresponding to the (111), (200), (220), and (311) surface, can be ignored before activation and when the sample was activated at 680 °C for 600 min, but they are very clear when the sample was activated at 740 °C for 480 min. This suggests that the cerium oxide is a fine particle and well dispersed on the carbon surface before activation, and will aggregate to larger particles during the activation process.

The SEM images of ACF-0, ACF-2, and ACF-4 are displayed in Fig. 4. There is no much difference between the ACF-0 and ACF-2. The spots on the ACFs may due to the dust adsorbed on the surface of fibers. However, carbon surface is rough and some drop-liquids are formed in ACF-4, it suggests that the cerium oxide etches the carbon surface and fuses to form larger particles during steam activation.

The adsorptions of Congo red and VB12 on ACFs from solutions are shown in Fig. 5. It will take longer time to reach equilibrium when the sample has broader pore size distribution. The ACF-4 exhibited the fastest adsorption rate and the biggest amount adsorbed among all samples. This is due to its largest mesoporous volume. The ACF-3 shows higher adsorption capacity of Congo red and VB12 than the ACF-1 and ACF-2 do because it has larger mesoporous volume and broader pore size. VB12 with larger molecular volume cannot be efficiently adsorbed on the pores of ACF-0 due to its less mesopore volume. The pore volume that is larger than the molecule volume determined the adsorption capacity and the adsorption rate was affected by the pore size distribution.

In summary, the mesopore in ACF can be developed by steam activation with cerium oxide; the micropore volume changes in limited degree, the mesopore increased is concentrated less than 5 nm. SEM showed that the fiber surface was rough and some liquid-shape was formed after activation with cerium oxide. The resulted ACF has larger adsorption capacity of Congo red and vitamin B12 due to its larger mesopore volume and wider pore diameter.

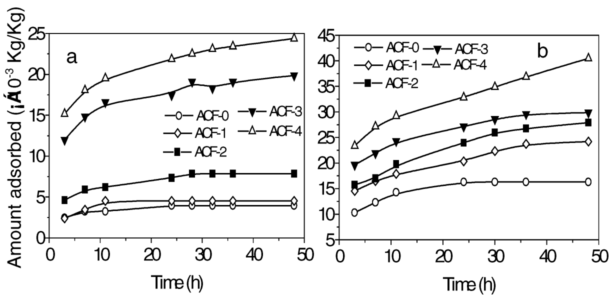

Figure 5 Adsorption capacities of Congo red: (a) and VB12 (b) on samples.

References

1. R. R. LJUBISA, in "Chemistry and Physics of Carbon," edited by R. R. Ljubisa (New York, 2001) Vol. 27, p. 228.
2. R. R. LJUBISA and S. CHAKKA, in "Introduction to Carbon Technologies," edited by H. Marsh, E. A. Heintz and F. Rodriguez-Reinoso (Universidad de Alicante, 1997) p. 103.
3. J. DIAZ-TERAN, D. M. NEVSKAIA, A. J. LOPEZ-PEINADO and A. JEREZ, *Colloid Surfaces* A **187/188** (2001) 167.
4. A. OYA, S. YOSHIDA, H. ALCANIZ-MONGE and A. LINAR-SOLANO, *Carbon* **8** (1995) 1085.
5. J. J. FREEMAN, F. G. R. GIMBLETT, R. A. ROBERTS and K. S. W. SING, *ibid.* **1** (1988) 7.
6. H. TAMAI, S. KOJIMA, M. IKEUCHI, J. MONDORI, T. KANATA and H. YASUDA, *TANSO (Jap.)* **175** (1996) 243.
7. E. H. HONG, Y. H. JUNG and K. H. LEE, *Korean J. Chem. Eng.* **2** (2000) 237.
8. F. RODRIGUEZ-REINOSO, in "Fundamental Issues in Control of Carbon Gasification Reactivity," edited by J. Lahaye and P. Ehrburgor (Boston, 1991) p. 533.
9. H. TAMAI, T. KAKII, Y. HIROTA, T. KUMAMOTO and H. YASUDA, *Chem. Mater.* **2** (1996) 454.
10. A. TOMITA, K. HIGASHIYAMA and Y. TAMAI, *Fuel* **2** (1981) 103.
11. H. TAMAI, M. IKEUCHI, S. KOJIMA and H. YASUDA, *Adv. Mater.* **1** (1997) 55.
12. Y. F. Y. YAO, *J. Catal.* **2** (1984) 152.
13. W. Z. SHEN, J. T. ZHENG, Z. F. QIN and J. G. WANG, *J. Colloid Interf. Sci.* **264** (2003) 467.
14. S. KASAOKA, Y. SAKATA, E. TANAKA and R. NATION, *Int. Chem. Eng.* **4** (1989) 734.
15. K. W. SING, D. H. EVERETT, R. A. W. HAUL, L. MOSCOU, R. A. PIEROTTI, J. ROUQUERO and T. SIEMIENIEWASA, *Pure Appl. Chem.* **5** (1985) 603.

Received 10 November 2003
and accepted 1 April 2004